ingegneria sismica
International Journal of Earthquake Engineering
Anno XLIII - Num. 3 - 2026

Design of Adaptive Overtorsion Sliding Mode Observer Based on Logarithmic Gain Law and Estimation of Satellite Disturbance Torque

Xu Yin[1,*] *and Yuhui Deng*[2]

[1] Shanghai Dianji University, Shanghai 201306, China
[2] Paisat Information Technology Co., Ltd., Shanghai, USA

SUMMARY: *Accurately estimate the real-time disturbance torque in the environment to improve the attitude control performance of the spacecraft. Based on flight data from a low-Earth-orbit satellite, an adaptive super-twisting sliding-mode observer (AST-SMO) is developed in this study, which integrates Kalman-filtered Euler-angle preprocessing for quasi-steady interval identification, adaptive band-pass filtering for angular-acceleration estimation, and a super-twisting observer with a state-dependent logarithmic gain law and dual leakage terms for chatter suppression. Compared with a fixed-gain observer, this one has a lower noise level and is more stable. The proposed observer improves the accuracy of disturbance-torque estimation and provides a practical basis for robust attitude-controller design.*

KEYWORDS: *adaptive super-twisting observer; sliding-mode observer; logarithmic gain law; disturbance torque estimation; satellite attitude control*

1 Introduction

Sources of disturbance torques for spacecraft attitude deviation in attitude control include gravity-gradient torque, atmospheric drag, solar radiation pressure and residual magnetic torque [1]. Real-time estimation of these torques can improve the disturbance rejection performance of attitude-control laws and support fault diagnosis and fault-tolerant control to enhance the reliability and service life of the system [2]. Existing estimation methods either model each source of disturbance independently or group the unknown effects into a single lumped disturbance term; this paper will use the latter form. Early in-orbit estimation studies used Kalman filtering for attitude and disturbance reconstruction. Markley and Sedlak added momentum-error states to spinning-spacecraft attitude estimation [3], and Soken and Hajiyev used an unscented Kalman filter to estimate microsatellite attitude dynamics in conjunction with solar and drag torques [4]. Disturbance observers (DOBs) do not need detailed modelling of the environment and are thus suitable for uncertain operating conditions. Hu and others have presented a finite-time DOB for rigid-spacecraft attitude control in the presence of input saturation [5]. To address the slow convergence and chattering of DOB and extended-state-observer structures, later research introduced sliding-mode mechanisms, particularly the second-order super-twisting algorithm. Yan and Wu have developed composite disturbances for flexible-spacecraft attitude stabilization [6], and other strong-perturbation nonlinear systems have shown the general applicability of this observer class through adaptive super-twisting ESO designs [7]. Classical super-twisting observers have fixed gains and are used to estimate

*13083430322@168.com
https://doi.org/10.65102/is20261245
Published: 10 June, 2026

bounded uncertainties in second-order sliding mode control [8]. Recent covariance analysis and studies on coupled disturbance-force measurement have also shown that stochastic and coupled disturbance components can affect attitude deviation, and thus need to be included in the estimation-oriented formulation [9, 10]. Fixed-gain schemes are trade-offs between convergence speed and chatter. To reduce this trade-off, a state-dependent logarithmic gain is introduced in the super-twisting observer in this paper. The gain increases smoothly during a large-error transient via a log1p-type function and returns to near the reference value at steady state to reduce chattering. On-orbit data verification shows that the initial stabilisation speed and low-frequency variations of the torque are both higher than those of the linear-gain benchmark.

2 System Modeling and Description

The angular dynamics around the centre of mass for the attitude control and environmental disturbance estimation of a three-axis stabilized satellite can be expressed as shown in Equation (1) by the rigid body Euler equation.

$$\mathrm{I}\dot{\omega}+\omega\times\left(\mathrm{I}\omega\right)=\mathrm{T}_{\mathrm{ctrl}}+\mathrm{T}_{\mathrm{dist}} \tag{1}$$

As shown in Equation (1), I is the inertia matrix of the satellite about the body-fixed axes, ω is the angular velocity in the inertial frame, $\mathrm{T}_{\mathrm{ctrl}}$ is the known control torque produced by flywheels or magnetorquers, and $\mathrm{T}_{\mathrm{dist}}$ is the unknown environmental disturbance torque caused by atmospheric drag, geomagnetic effects, solar radiation pressure and other orbital disturbances.

2.1 Definition and Estimation Objectives

Environmental disturbance torques change slowly and have small high-frequency fluctuations. The aim is to build an observer output that has a finite-time converging estimation error or is within an acceptable chattering bound under measurement noise.

3 Methodology Design

3.1 Input Preprocessing

Angular Velocity Conversion

Discrete Euler-angle sequences of spacecraft telemetry are smoothed using a Savitzky-Golay filter with a 15-point window and a cubic polynomial. Then, numerically differentiate the angular velocity to obtain angular acceleration. Assuming the 3-2-1 rotation sequence, Equation (2) is used to obtain the body-frame angular velocity.

$$\boldsymbol{\omega}_k=\underbrace{\begin{bmatrix}1 & 0 & -\sin\tilde{\theta}_k\\ 0 & \cos\tilde{\varphi}_k & \sin\tilde{\varphi}_k\cos\tilde{\theta}_k\\ 0 & -\sin\tilde{\varphi}_k & \cos\tilde{\varphi}_k\cos\tilde{\theta}_k\end{bmatrix}}_{T\left(\tilde{\varphi}_k,\tilde{\theta}_k\right)}\begin{bmatrix}\dot{\tilde{\varphi}}_k\\ \dot{\tilde{\theta}}_k\\ \dot{\tilde{\psi}}_k\end{bmatrix} \tag{2}$$

Equation (2) is used to convert the Euler-angle rate vector into a body-frame angular-velocity vector.

First-Order Kalman Smoothing

A one-dimensional Kalman filter is constructed for the angular velocity of each channel $\omega_{j,k}$ obtained in the previous step:

$$\begin{aligned} p_k &= p_{k-1} + q, \\ K_k &= \frac{p_k}{p_k + r}, \\ \hat{\omega}_{j,k} &= \hat{\omega}_{j,k-1} + K_k\left(\omega_{j,k} - \hat{\omega}_{j,k-1}\right), \\ p_k &\leftarrow \left(1 - K_k\right) p_k \end{aligned} \tag{3}$$

q and r are the process-noise and measurement-noise covariances, respectively, here. The filtered output is the smoothed angular velocity used for acceleration estimation in the following steps.

Angular Acceleration Estimation

The Savitzky-Golay filter is used once more to obtain the higher-order derivatives of the smoothed angular-velocity sequence. First-order differencing yields angular acceleration; thus, upper- and lower-bound clipping are used to ensure numerical stability of the acceleration estimate.

Calculation of Environmental Torque Components

Model IGRF13 of the geomagnetic field is used to calculate magnetic torque. Then, Euler dynamics are inverted to obtain the environmental disturbance-torque sample by subtracting the known control and magnetic-torque components.

3.2 Logarithmic adaptive super-twisting sliding-mode observer

To estimate environmental disturbance torque, an adaptive super-twisting sliding-mode observer with dual state vectors is used. The state vectors are the first-order disturbance estimate and the sliding-mode compensation term. The estimation error is divided into components ej, and a leakage coefficient is added to introduce damping in the near-zero-error region to suppress high-frequency jitter. To balance convergence speed and vibration suppression, a logarithmic gain law that changes according to the size of the error is used [11, 12]:

$$k_{1,j}^{des} = K_{1,0} + \Gamma_1 ln\left(1 + \left|e_j\right|\right), \quad k_{2,j}^{des} = K_{2,0} + \Gamma_2 ln\left(1 + \left|e_j\right|\right) \tag{4}$$

$k_{1,0}$ and $k_{2,0}$ are the reference gains in Equation (4), and a_1 and a_2 are the gain-adjustment rates. Since $ln(1+|e_j|)$ is an increasing function of $|e_j|$, the observer increases the gain during a large-error transient and returns it to the reference value near steady state to reduce chatter.

At each sampling point, the actual gain is smoothed towards the expected gain by the smoothing factor:

$$k_{1,j}^{+} = k_{1,j} + \alpha\left(k_{1,j}^{\text{des}} - k_{1,j}\right) \quad , k_{2,j}^{+} = k_{2,j} + \alpha\left(k_{2,j}^{\text{des}} - k_{2,j}\right) \tag{5}$$

The adaptive super-twisting sliding-mode update law is expressed as:

$$\dot{d}_j = -K_{1,j} sgn\left(e_j\right)\sqrt{\left|e_j\right|} + v_j - \lambda d_j \tag{6}$$

$$\dot{v}_j = -K_{2,j} sgn\left(e_j\right) - \lambda v_j \tag{7}$$

In Equations (6) and (7), j = 1, 2, 3 are the three body-axis channels, and sgn(.) is the sign function.

For numerical stability, the continuous sliding-mode observer equations are integrated using the classical fourth-order Runge-Kutta (RK4) method, and the discrete update at sampling step h is as follows:

$$\begin{aligned} \boldsymbol{d}_{k+1} &= \boldsymbol{d}_k + \frac{h}{6}\left(\boldsymbol{k}_1 + 2\boldsymbol{k}_2 + 2\boldsymbol{k}_3 + \boldsymbol{k}_4\right), \\ \boldsymbol{v}_{k+1} &= \boldsymbol{v}_k + \frac{h}{6}\left(\ell_1 + 2\ell_2 + 2\ell_3 + \ell_4\right), \end{aligned} \tag{8}$$

The four evaluation increments of RK4 are determined at the four intermediate points. This discrete form still has the high-order error-suppression property of the super-twisting observer and is robust to finite-precision computation.

3.3 Convergence Proof of the Adaptive Logarithmic Gain

The convergence analysis is based on the continuous-time observer form in Equation (9), and a strict Lyapunov construction is employed for super-twisting algorithms [13].

$$\begin{cases} \dot{d}_j = -k_{1,j}\left(e_j\right) sgn\left(e_j\right)\sqrt{\left|e_j\right|} + v_j - \lambda d_j, \\ \qquad \dot{v}_j = -k_{2,j}\left(e_j\right) sgn\left(e_j\right) - \lambda v_j, \end{cases} e_j = d_j - T_j,\ j \in x, y, z \tag{9}$$

Set up a Lyapunov function as:

$$V = \sum_{j=1}^{3}\cdot\left(\frac{1}{2}e_j^2 + \frac{1}{2}k_{1,j}v_j^2\right) \tag{10}$$

The logarithmic gain is given by Equation (4), and the actual gain is updated according to the following exponential smoothing law:

$$\dot{k}_{i,j} = \alpha\left(k_{i,j}^{\text{des}} - k_{i,j}\right), i = 1, 2, \alpha \in (0,1) \tag{11}$$

As the size of the error increases, so does the logarithmic term; at the same time, the smoothing update maintains a positive and bounded adaptive gain.

Differentiating the Lyapunov function and substituting the observer dynamics gives the following expression after omitting the channel subscript j:

$$\dot{V} = e\dot{e} + \frac{1}{2}\dot{k}_1 v^2 + k_1 v\dot{v} \tag{12}$$

The residual terms are regarded as bounded small disturbances after front-end low-pass filtering, and the remaining high-frequency components are neglected. Substitute Equations (9) and (11) to obtain:

$$\begin{aligned}\dot{V} &= e\left(-k_1 sgn(e)\sqrt{|e|} + v - \lambda d - \hat{T}\right) + \frac{1}{2}\alpha\left(k_1^{\text{des}} - k_1\right)v^2 + k_1 v\left(-k_2 sgn(e) - \lambda v\right) \\ &\le -k_1|e|^{\frac{3}{2}} + ev - \lambda e^2 - k_1 k_2 v sgn(e) - \lambda k_1 v^2 + \frac{1}{2}\alpha\Gamma_1 ln\left(1+|e|\right)v^2 + (\text{Small disturbance term})\end{aligned} \tag{13}$$

Based on the inequality in Equation (14), a suitable β value can be chosen, and the result is:

$$-k_1|e|^{\frac{3}{2}} - k_1 k_2 v sgn(e) \le -c_1 e^2 - c_2 v^2 \tag{14}$$

The dead zone is used to suppress the attenuation of the residual estimation error in the small-error region. In the large-error region, the amplified logarithmic-gain term can be used to select the corresponding coefficients so that:

$$\dot{V} \le -c\left(e^2 + v^2\right), c > 0 \tag{15}$$

The two regions lead to a single negative-definite Lyapunov derivative, and thus the three-channel observer is globally and exponentially convergent. If a fractional-order Lyapunov function with an exponent of $0 < \alpha < 1$ is selected, finite-time convergence can also be achieved.

The adaptive logarithmic-gain super-twisting sliding-mode observer is thus a combination of near-zero-error damping, smooth logarithmic-gain adjustment and sliding-mode compensation. The above Structure is relatively immune to small errors and exhibits fast-convergence behaviour for large departures, thereby meeting the real-time disturbance-torque-estimation needs of the current spacecraft.

4 Analysis of Results for Satellite Environmental Disturbance-Torque Estimation

4.1 Calculation Method and Evaluation Indicators

Attitude-control data from small satellites at an altitude of 300-400 km are used, which include UTC timestamps, inertial three-axis angular velocities, magnetic torques and wheel torques. First, the quasi-steady segments are identified and kept; then, the abrupt-change intervals are excluded before smoothing and filtering. The inertia tensor of the satellite is diag([180.0, 185.0, 238.0]) $kg \cdot m^2$.

Four indicators are used to evaluate the algorithms: convergence speed, the number of steps needed for the error to enter and stay within the steady-state tolerance; steady-state error, which is the mean plus or minus the standard deviation over the second half of the run; robustness, measured by the range between the maximum and minimum steady-state torque norms; and computational cost, which is calculated as the total execution time divided by the number of steps in ms/step [14].

4.2 Results Comparison

Table 1 is the same for both the linear-gain and logarithmic-gain observers in the telemetry section. Comparison of convergence, steady-state error, torque fluctuation, average control torque and single-step computational cost.

Table 1: Comparison of linear and logarithmic gain methods.

Indicator	Linear gain	Logarithmic gain	Interpretation
Convergence steps	200 (err<0.0012)	310 (err<0.0013)	Linear gain reaches final tolerance faster.
Steady-state error	0.0009±0.0002 N·m	0.0009±0.0002 N·m	Accuracy is comparable.
Torque range	0.0007-0.0821 N·m	0.0004-0.0779 N·m	Range is reduced by 47%.
Average torque	0.003760 N·m	0.004426 N·m	Difference remains small.
Single-step cost	0.0760 ms/step	0.0740 ms/step	Computational cost is comparable.

Figure 1 shows the error-norm paths of the two observers. The first 100 steps show that the logarithmic-gain observer has reduced the state-error norm to 0.04 and, by this time, surpassed the linear-gain observer's value of 0.05 by 20 per cent. Although full convergence requires 310 steps instead of 200, the logarithmic-gain observer has a smaller early-stage error and is thus more suitable for the initial attitude-control transient.

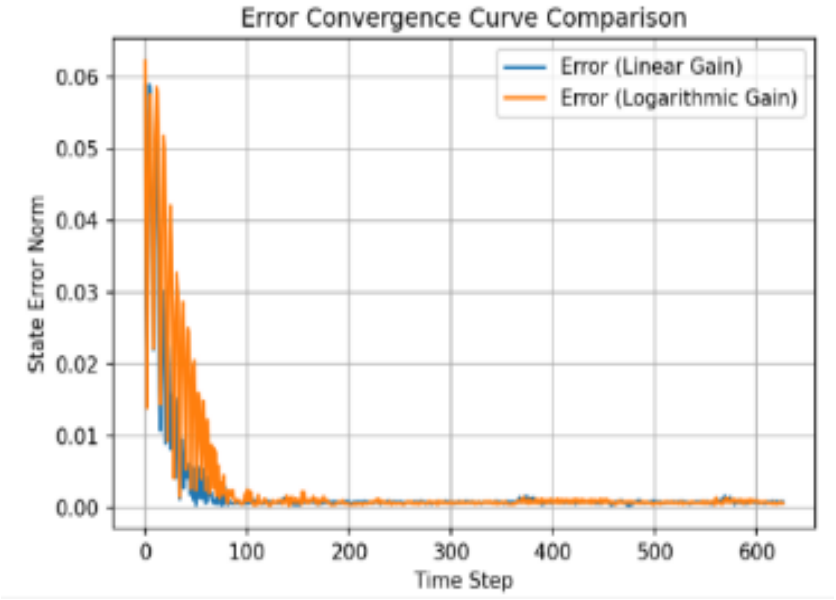

Figure 1: Comparison of Error Convergence Curves.

Figure 2 is the steady-state torque distribution. The logarithmic-gain observer has an interquartile range of 0.0005 N*m, with Q1 = 0.0018 N*m and Q3 = 0.0023 N*m; this value is half that of the 0.0010 N*m interquartile range for the linear-gain observer. A narrow distribution indicates that high-frequency torque buffeting is suppressed more strongly and steady-state estimation is more stable.

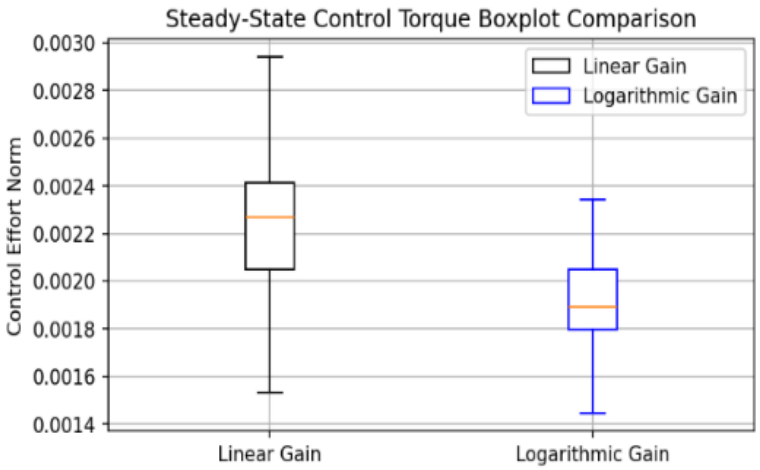

Figure 2: Steady-State Control Torque Boxplot Comparison.

Figure 3 is the observer-gain dynamics. In the first 500 steps, the peak-to-peak swing of the linear gain k_1 is about 0.012, and the change in logarithmic gain is less than 0.001 per step. A gradual rise and fall are to avoid the overmodulation of a fixed-gain sliding-mode observer.

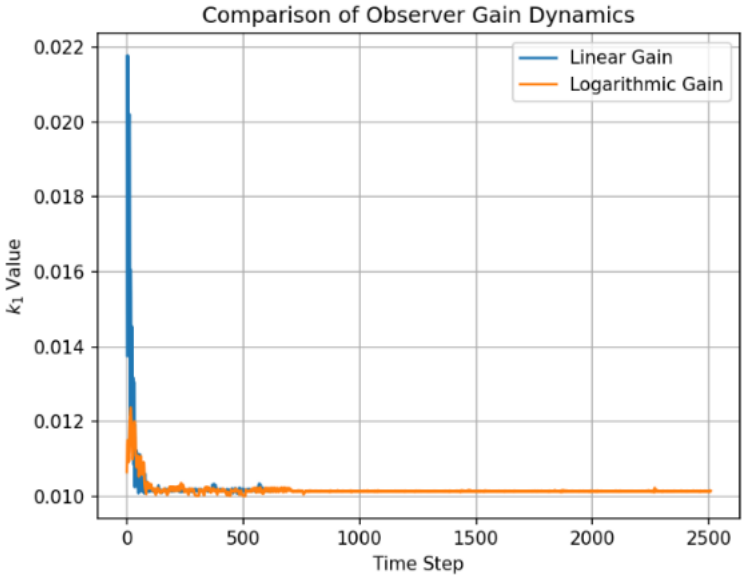

Figure 3: Observer-gain Dynamics Comparison.

5 Summary

The proposed logarithmic-gain adaptive super-twisting sliding-mode observer can reduce the initial error more quickly, decrease torque fluctuations, and exhibit stable parameter behaviour for satellite environmental disturbance-torque estimation. It has the same steady-state accuracy and computation cost as the classical linear-gain scheme but reduces steady-state torque variation. Further optimise the gain-adjustment rate to improve estimation accuracy under more complex time-varying disturbance conditions. Therefore, the proposed disturbance-torque estimation method is also suitable for manoeuvring-control and attitude-control design of small satellites.

References

[1] Yang, Y. (2019). Spacecraft Modeling, Attitude Determination, and Control: Quaternion-Based Approach. CRC Press.

[2] Wang, N., Hamrah, R., Sanyal, A. K., & Glauser, M. N. (2023). Geometric extended state observer on SE(3) with fast finite-time stability: Theory and validation on a rotorcraft aerial vehicle. arXiv preprint arXiv:2307.08762.

[3] Markley, F. L., & Sedlak, J. E. (2008). Kalman filter for spinning spacecraft attitude estimation. Journal of Guidance, Control, and Dynamics, 31(6), 1750-1760.

[4] Soken, H. E., & Hajiyev, C. (2014). Estimation of pico-satellite attitude dynamics and external torques via unscented Kalman filter. Journal of Aerospace Technology and Management, 6(2), 149-157.

[5] Hu, Q., Li, B., & Qi, J. (2014). Disturbance observer based finite-time attitude control for rigid spacecraft under input saturation. Aerospace Science and Technology, 39, 13-21.

[6] Yan, R., & Wu, Z. (2019). Super-twisting disturbance observer-based finite-time attitude stabilization of flexible spacecraft subject to complex disturbances. Journal of Vibration and Control, 25(5), 1008-1018.

[7] Ma, R., Siaw, F. L., Thio, T. H. G., & Yang, W. (2024). New adaptive super-twisting extended-state observer-based sliding mode scheme with application to FOWT pitch control. Journal of Marine Science and Engineering, 12(6), 902.

[8] Davila, J., Fridman, L., & Levant, A. (2005). Second-order sliding-mode observer for mechanical systems. IEEE Transactions on Automatic Control, 50(11), 1785-1789.

[9] Obama, B. N. V. A., Shi, P., Saeed, A., Hassen, A. Y., & Sanusi, B. M. (2023). Study on attitude deviation of spacecraft subjected to random disturbance torque based on covariance analysis. Journal of Physics: Conference Series, 2512(1), 012013.

[10] Zhou, C., Xu, Z., & Xia, M. (2024). Prediction technique and measuring device for coupled disturbance forces from large equipment in the spacecraft. Sensors, 24(4), 1284.

[11] Li, Y., Tan, P., Liu, J., & Chen, Z. (2022). A super-twisting extended state observer for nonlinear systems. Mathematics, 10(19), 3584.

[12] Winkler, A., Grabmair, G., & Reger, J. (2023). On implementing the implicit discrete-time super-twisting observer on mechanical systems. International Journal of Robust and Nonlinear Control, 33(13), 7532-7562.

[13] Moreno, J. A., & Osorio, M. (2012). Strict Lyapunov functions for the super-twisting algorithm. IEEE Transactions on Automatic Control, 57(4), 1035-1040.

[14] Xu, G., Luo, S., Huang, Y., & Deng, X. (2025). Extended state observer based robust nonlinear PID attitude tracking control of quadrotor with lumped disturbance. Processes, 13(5), 1470.